22nd International Conference on Renewable Energies and Power Quality (ICREPQ'24)
Bilbao (Spain), 26th to 28th June 2024
Renewable Energy and Power Quality Journal (RE&PQJ)
ISSN 2172-038 X, Volume No.22, September 2024

4D hybridisable interpolation methodology aimed at system modelling: application to a fuel cell blower

J. Rodriguez-Gongora[1], F.J. Asensio[1], A. Ordono[1], M. Gonzalez-Perez[1], G. Saldaña[2], O. Oñederra[2]

[1] Department of Electrical Engineering
Engineering School of Gipuzkoa, University of the Basque Country (UPV/EHU)
Avda. Otaola, 29, 20600 Eibar (Spain)
Phone/Fax number: +34 943 033014

[2] Department of Electrical Engineering
Engineering School of Bilbao, University of the Basque Country (UPV/EHU)
Pza. Ingeniero Torres Quevedo, 1, 48013 Bilbao (Spain)
Phone/Fax number: +34 946 014367

Abstract.

This paper focuses on providing an empirical model construction methodology based on Piecewise Cubic Hermite Interpolation Polynomials (PCHIP). The proposed methodology is suitable for modelling systems with high non-linearity between system parameters, process variables and/or operation variables. A detailed description of the 4D interpolation methodology is given and a practical application for a fuel cell (FC) blower black-box model obtaining is shown. The results of the algorithm-based model are compared to datasheet specifications to validate the FC blower model. The validation shows a good precision in the operation limits estimation. Additionally, some FC-related applications suitable for the obtained blower model utilization are described.

Key words. Piecewise Cubic Hermite Interpolation Polynomials (PCHIP), Modelling, Fuel Cells (FC), Blower.

1. Introduction

In recent years, hydrogen Fuel Cell (FC) technology has become one of the technologies with the best future prospections, as a result of its wide range of applications **[1]**. Some of the fields with increasing FC presence are Combined Heat and Power systems (CHP), Electric Vehicle (EV), and microgrids based on Renewable Energy Sources (RES) **[2]**.

To ensure a proper FC system design, control and management, models of the plant and the auxiliary components are required. Existing model construction methods can be classified in two main groups.

On the one hand, mechanic-analytical models based on Computational Fuel Cell Dynamics (CFCD) **[3-4]** achieve high accuracy, but the elevated computational cost makes them unsuitable for real-time applications. Additionally, they require an expensive powerful computational hardware, which is not usually affordable for low-power non-industrial applications.

On the other hand, semiempirical or empirical models **[5]** have the advantage of short computational time, due to the system model simplicity in terms of variables and mathematical correlations. This often leads to poor system response predictions, which might be unacceptable depending on the application.

Hybrid models **[6]** are expected to be a good solution to achieve a good trade-off between accuracy and computational cost and time. A feasible method for a hybrid model construction would be to combine empirical models for the FC subsystems and an analytical model for the FC stack.

The aim of this work is to provide an empirical model construction method based on Piecewise Cubic Hermite Interpolation Polynomials (PCHIP) for systems with high non-linearity between system parameters, process variables and/or operation variables.

The structure of this paper is as follows. Section 2 provides a detailed description of the modelling methodology, both of PCHIP and the interpolation algorithm. Section 3 shows the results of the model obtaining method for a commercial FC blower. In Section 4 the FC blower model is validated, comparing predictions to datasheet. Section 5 focuses on the description of some application cases of the obtained model. Finally, conclusions are exposed in Section 6.

2. 4D Modelling Methodology

The methodology used to create a suitable 4-interdependent-variable model is based on Shape-Preserving Cubic Spline methods, namely PCHIP.

A. PCHIP

What characterizes PCHIP among other piecewise cubic interpolating polynomials is how the coefficients of polynomials are calculated. PCHIP are given by a unique polynomial satisfying the following conditions for every internal interval $[\boldsymbol{x_i}, \boldsymbol{x_{i+1}}]$ **[7]**:

1) First Condition

$$\boldsymbol{P_i(x_i) = f(x_i)} \tag{1}$$

$$\boldsymbol{P_i(x_{i+1}) = f(x_{i+1})} \tag{2}$$

2) Second Condition

$$\boldsymbol{\frac{dP_i}{dx}(x_i) = f'(x_i)} \tag{3}$$

$$\boldsymbol{\frac{dP_i}{dx}(x_{i+1}) = f'(x_{i+1})} \tag{4}$$

The first condition ensures that the image of the interpolating polynomial coincides with that of the given setpoints. The second condition, on the other hand, restricts the slope of the resulting polynomial curve in the given setpoints. By doing this, the continuity of the first derivative of the polynomial curve is achieved and the monotonicity of the adjustment curve can be guaranteed **[6].**

The slope of the function in the given points is usually unknown. This leads to the need of an approximation method for estimating the tangents $\boldsymbol{m_i}$ of the function. The most used method is the Fritsch-Carlson method given by (5). Additionally, to respect the monotonicity of the resulting curve, that is, the curve is strictly increasing or decreasing, the estimated tangent value $\boldsymbol{m_i}$ must be modified according to the sign of the secants as shown in (5) and (6).

$$\boldsymbol{m_i = \frac{1}{2} \cdot (\delta_i + \delta_{i-1}) \quad if\ sign(\delta_{i-1}) = sign(\delta_i)} \tag{5}$$

$$\boldsymbol{m_i = 0 \quad if\ sign(\delta_{i-1}) \neq sign(\delta_i)} \tag{6}$$

where:
- δ_i is the slope of the secant line between the considered and the succeeding points given by (7).
- δ_{i-1} is the slope of the secant line between the considered and the preceding points given by (8).

$$\boldsymbol{\delta_i = \frac{f(x_{i+1}) - f(x_i)}{x_{i+1} - x_i}} \tag{7}$$

$$\boldsymbol{\delta_{i-1} = \frac{f(x_i) - f(x_{i-1})}{x_i - x_{i-1}}} \tag{8}$$

Finally, the mathematical expression of each piecewise polynomial P_i for a given internal interval $[x_i, x_{i+1}]$ as a function of the estimated tangent m_i and the data points $(x_i, f(x_i))$ is shown in (9) [8].

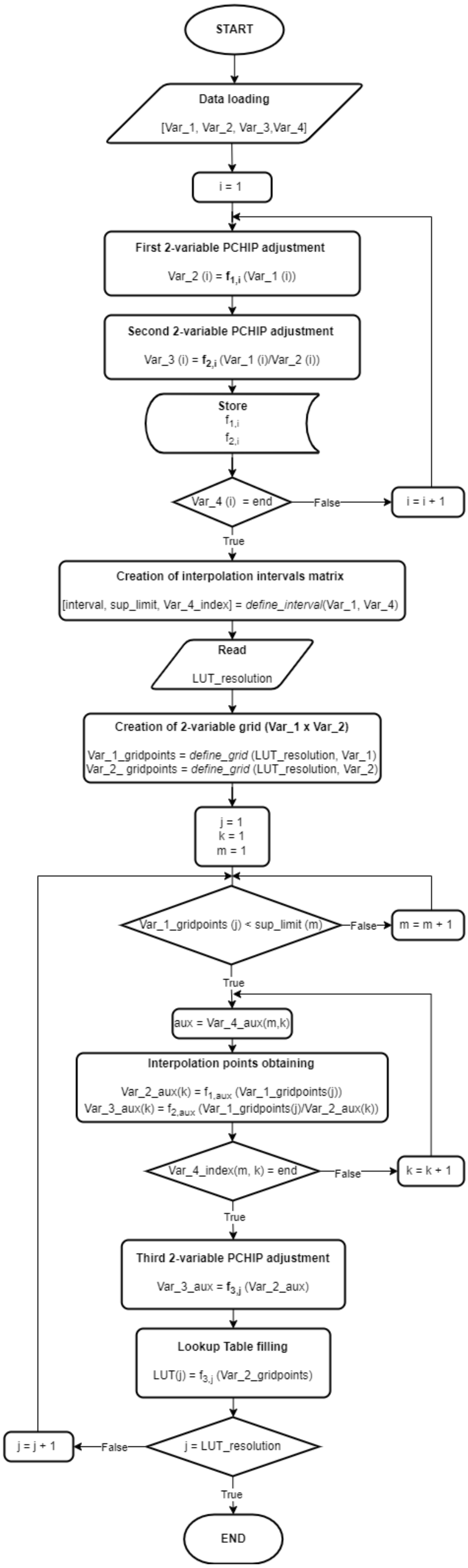

Figure 1. Lookup table construction algorithm.

$$P_i(x) = h_{00}(t) \cdot f(x_i) + h_{10}(t) \cdot (x_{i+1} - x_i) \cdot m_i + \boldsymbol{h_{01}(t) \cdot f(x_{i+1}) + h_{11}(t) \cdot (x_{i+1} - x_i) \cdot m_{i+1}} \quad (9)$$

where:

- $h_{00}(t), h_{10}(t), h_{01}(t)$ and $h_{11}(t)$ are the Hermite basis functions dependent on t, which stands for the normalization of the x variable to the interval length, whose values are comprised between 0 and 1 for the initial and final points of the interval, respectively.

B. 4D Interpolation Algorithm

Since PCHIP may only be used for correlation between two variables, it has been necessary to establish a methodology to interpolate among 4 variables. The flowchart of the algorithm used for the construction of a four-dimension lookup table is presented in Fig. (1).

The first steps of the presented algorithm consist of adequately correlating the four input variables. This is achieved by the first and second PCHIP adjustments. Next, the interpolation intervals for the lookup table creation are defined according to the independent variable for the interpolation (*Var_1*) and the variable which has not been directly related to the other ones (*Var_4*). This is compulsory when input data are unevenly scattered.

Before the iterative processes of interpolation and lookup table (LUT) fulfilling, the so-called grid of the LUT must be defined. It is a square matrix of a number of elements according to the user defined variable *LUT_resolution*. The row number corresponds to a certain value of *Var_1* defined by the vector *Var_1_gridpoints*, whereas the column number corresponds to a certain value of *Var_2* specified by the vector *Var_2_gridpoints*. Thus, the matrix is eventually filled with the interpolated values of *Var_3*.

Although the flowchart of the algorithm only shows the creation of a LUT where *Var_1*, *Var_2* and *Var_3* are correlated, the same process would be carried out to interrelate *Var_4* with *Var_1*, *Var_2* and/or *Var_3*.

To ensure a proper and truthful interpolation methodology based on the available input data, some auxiliary functions, indicated in cursive in Fig. (1), are needed. However, since they uniquely serve as a complement to the functioning of the algorithm, they are left out of the scope of this paper.

3. FC blower black-box model obtaining

The interpolation algorithm has been applied to the Eberspächer VAIREX VRB6-25 blower to obtain an extended operating-point model based on the datasheet

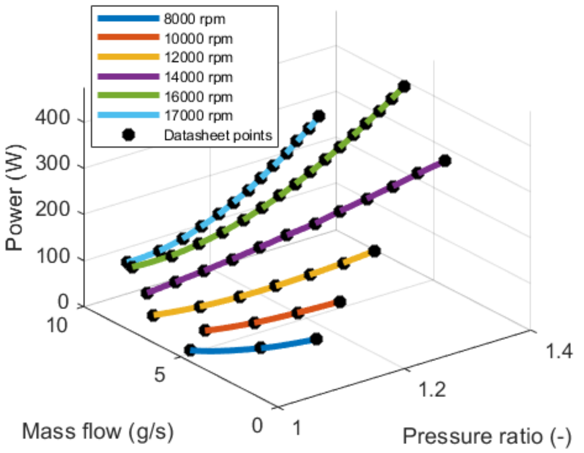

Figure 2. Interpolation results of first and second PCHIP adjustments for every blower speed.

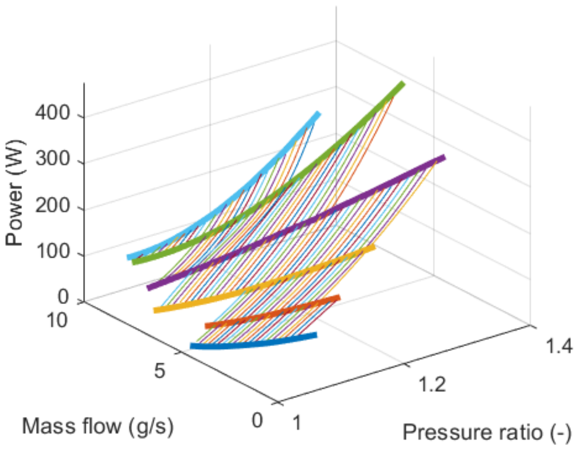

Figure 3. Graphical representation of third PCHIP adjustment.

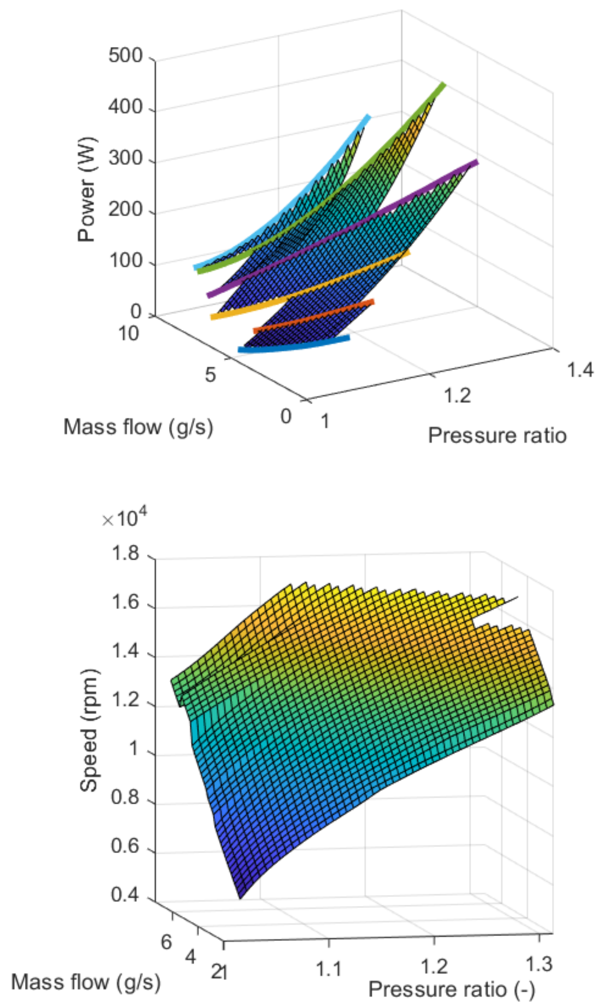

Figure 4. Interpolation algorithm results.

specifications **[9]**. The variables of interest for this type of application are the pressure ratio, the mass flow, the power consumption, and the rotational speed of the blower.

The previous figures summarize the interpolation steps and results. Fig. (2) shows the interpolated curves for every speed based on the blower datasheet points. Fig. (3) represents graphically with the thinner curves how the interpolation algorithm process is carried out to create a map of the operating points of the blower. Fig. (4) exposes graphically the interpolated values for the blower power consumption and the blower speed as a function of the mass flow and the pressure ratio.

4. Validation results

Due to the lack of the necessary equipment for the experimental verification of the algorithm predictions, it has been tested with the data specified in the datasheet. For the test, the 12,000 rpm-speed data have been deleted from the input of the algorithm.

Fig. (5) shows the model predictions faced to the datasheet specifications. The maximum relative errors obtained are: 4.86% for the power-pressure ratio interpolation; 8.76% for the power-mass flow interpolation and 3.77% for the pressure ratio-mass flow interpolation.

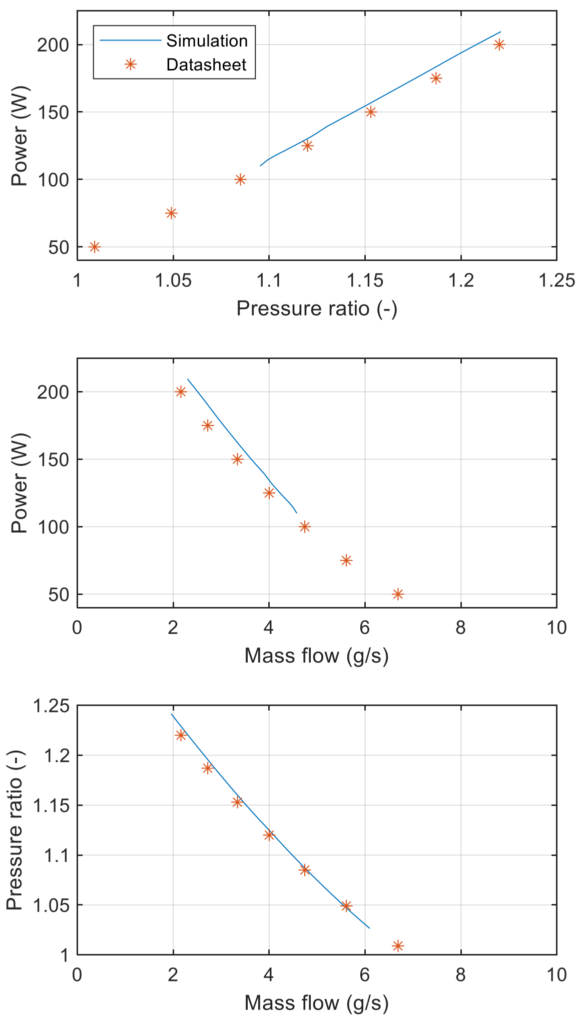

Figure 5. Predicted results vs datasheet.

5. Model application

This section describes some application cases where the developed FC blower model could be used. Firstly, an in-depth explanation to set the dynamic saturation of a PID controller is carried out. Secondly, other application approaches are introduced.

A. Dynamic saturation for PID controllers

In this subsection, it is deeply described how the obtained model can be used to stablish the saturation of PID controllers. The presented application case is further detailed in the following lines. Fig. (7) and (8) show the FC cathode air feeding system and the air humidity regulation schemes, respectively.

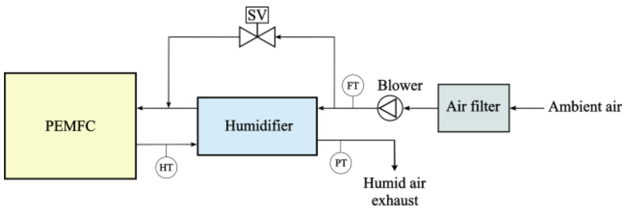

Figure 7. FC cathode air feeding system scheme.

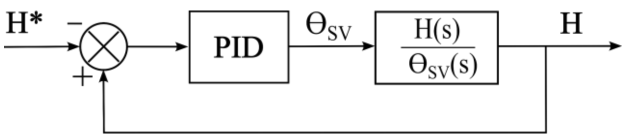

Figure 8. Air humidity regulation scheme.

The humidity control system works as follows. If the humidity transmitter (HT) detects an excessive percentage of humidity in the cathode air, the solenoid valve (SV) in parallel with the humidifier is slightly opened to reduce the air mass flow through the humidifier. The opposite is done if low humidity is detected.

The opening of the SV directly affects the pressure drop of the whole system, thus creating a perturbation on the mass flow control system. This may lead to an undesirable transitory, where oscillations in the air mass flow take place and output pressure operation limits are not always respected. To prevent this from occurring, a dynamic saturation based on the obtained FC blower black-box model is presented.

1) System pressure drop characterization

First, the system pressure drop must be characterized. In this case, the total pressure drop of the system can be summarized in the following expression:

$$\Delta p_{FC} = \Delta p_{fil} + \Delta p_{hum//SV} + \Delta p_{pip} + \Delta p_{FT} + \Delta p_{cath} \qquad \textbf{(10)}$$

where:
- Δp_{FC} is the total pressure drop across the FC cathode air feeding system.
- Δp_{fil} is the pressure drop across the air filter.

- $\Delta p_{hum//SV}$ is the pressure drop across the parallel connection of the humidifier and the SV.
- Δp_{pip} is the pressure drop across the pipes.
- Δp_{FT} is the pressure drop across the mass flow transmitter.
- Δp_{cath} is the pressure drop across the cathode air channels.

This expression can be further generalized separating the pressure-drop constant terms and the mass-flow-variable terms:

$$\boldsymbol{\Delta p_{FC} = k_{FC} \cdot \dot{m}^2 + constant} \qquad (\mathbf{11})$$

where:
- k_{FC} is the pressure drop coefficient of the air feeding system calculated according to (12).
- $\dot{m}$ is the air mass flow.

$$\boldsymbol{k_{FC} = k_{fil} + k_{hum//SV} + k_{pip} + k_{FT} + k_{cath}} \qquad (\mathbf{12})$$

Where every pressure drop coefficient corresponds to the aforementioned pressure drops in (10). The pressure drop coefficients can be easily obtained from the datasheet of the components, except for the pressure drop coefficient of the parallel of the humidifier and the SV, which is calculated according to (13).

$$\boldsymbol{k_{hum//SV} = \frac{k_{hum} k_{SV}}{\left(\sqrt{k_{hum}} - \sqrt{k_{SV}}\right)^2}} \qquad (\mathbf{13})$$

Considering the relation between the pressure drop coefficient of the SV ($\boldsymbol{k_{SV}}$) and its opening degree ($\boldsymbol{\theta_{SV}}$), the total pressure drop curve of the system as a function of the mass flow and the SV opening degree is achieved.

2) Operation limit curve obtention

Once the total pressure drop coefficient of the system is determined based on the individual coefficient values and the pressure-drop constant terms are known, the operation limit curve can be obtained. In Figs. (9) and (10) the intersection of the pressure drop curve with the operating point map of the FC blower is represented. For the pressure drop curve in this example, pressure drop constant terms have been neglected and a total pressure drop coefficient of 0.04 $(s/g)^2$ has been considered.

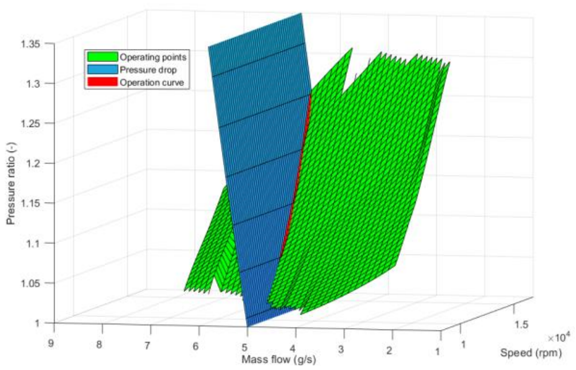

Figure 9. 3D graphic of the operation curve (intersection).

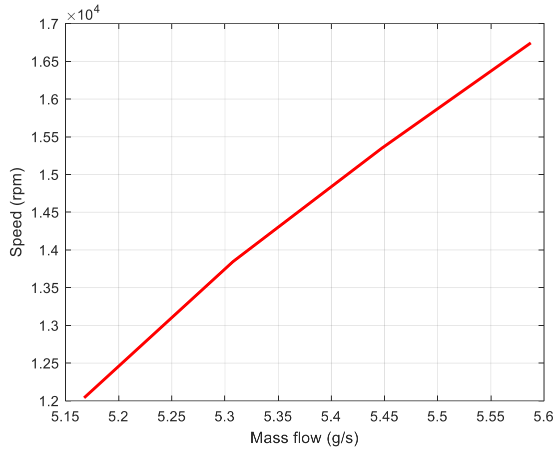

Figure 10. 2D graphic of the operation curve.

The obtained operation curve represents the set of operating points that respect operation limits for the given pressure drop curve of the system. Moreover, since these points establish a separation between the operating region where output pressure operation limits are guaranteed (upper region in Fig. (10)) and where they are not (lower region), the obtained curve can be used as a limiter to ensure the proper working conditions of the system.

3) Dynamic saturation implementation

Fig. (11) shows the mass flow control scheme with the implementation of the dynamic saturation. This block carries out the previously mentioned processes of total pressure drop curve determination and operation limit curve obtention. Then, the inferior limit value of the blower speed is selected according to the operation limit curve and the reference mass flow. Eventually, if PID output ever goes below the inferior limit value of the dynamic saturation block, the reference blower speed will stick to the limit value to ensure operation limits are always respected.

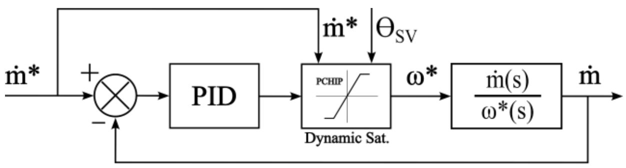

Figure 11. Mass flow control scheme with dynamic saturation.

B. Other application approaches

Control feedforward: lookup tables have already been proposed for control loop feedforwards in FCs **[10]** for faster control dynamics. However, the accuracy of the feedforward lookup table plays a crucial role in the achievement of faster control response. For that reason, PCHIP-based blower lookup table could be a good candidate for LUT-based feedforwards.

Blower black-box for pseudo-static simulation: considering the accuracy of the model stationary predictions, it could be implemented in long-step-time FC stack simulation for reduction of computational time and cost. For example, it could be helpful for FC component degradation analysis which have to simulate long-term pseudo-static conditions.

Blower fault detection: the predictions of the model can be used as reference for the state of health of the FC blower. Slight discrepancies must be tolerated during normal operation. However, big differences may indicate failure of the system.

Precise estimation of operation limits: in the design process of a FC stack, operation limits of the subsystems must be considered to determine whether they are suitable or not. Although linear interpolation can be used to estimate the behaviour of components, the presented model predictions can be more precise and helpful since 4 different variables are interrelated.

6. Conclusions

This paper has presented a 4D modelling methodology that has proven to be reliable for the stationary model of a FC blower.

A practical application case aimed at obtaining the operating curve of a FC blower is exposed. It is shown how the proposed methodology allows predicting whether the system will operate respecting the limits of maximum pressure drop in the cathode air supply system, depending on the process and control variables.

It has been introduced how the precise estimation of operation limits can also be useful in FC regulation schemes, namely as a dynamic saturation for PID controllers.

Finally, it should be noted that the proposed modelling methodology, in addition to precise estimation of operation limits, can be used in a wide range of applications, such as FC control optimization, FC degradation simulation or blower fault detection.

Acknowledgement

Authors thank for the support received from the Ministry of Industry and Tourism of Spain (grant for projects of hybrid vehicles and electric vehicles with batteries and hydrogen fuel cells, HIB-01-07-2023).

References

[1] N. Sazali, W. N. Wan Salleh, A. S. Jamaludin, y M. N. Mhd Razali, «New Perspectives on Fuel Cell Technology: A Brief Review», *Membranes*, vol. 10, n.º 5, p. 99, may 2020, doi: 10.3390/membranes10050099.

[2] Z. Li, Z. Zheng, L. Xu, y X. Lu, «A review of the applications of fuel cells in microgrids: opportunities and challenges», *BMC Energy*, vol. 1, n.º 1, p. 8, dic. 2019, doi: 10.1186/s42500-019-0008-3.

[3] C.-Y. Wang, «Fundamental Models for Fuel Cell Engineering», *Chem. Rev.*, vol. 104, n.º 10, pp. 4727-4766, oct. 2004, doi: 10.1021/cr020718s.

[4] F. J. Asensio, J. I. San Martín, I. Zamora, G. Saldaña, y O. Oñederra, «Analysis of electrochemical and thermal models and modeling techniques for polymer electrolyte membrane fuel cells», *Renew. Sustain. Energy Rev.*, vol. 113, p. 109283, oct. 2019, doi: 10.1016/j.rser.2019.109283.

[5] J. Wishart, Z. Dong, y M. Secanell, «Optimization of a PEM fuel cell system based on empirical data and a generalized electrochemical semi-empirical model», *J. Power Sources*, vol. 161, n.º 2, pp. 1041-1055, oct. 2006, doi: 10.1016/j.jpowsour.2006.05.056.

[6] S. Ou y L. Achenie, «A hybrid neural network model for PEM fuel cells», *J. Power Sources*, vol. 140, n.º 2, pp. 319-330, feb. 2005, doi: 10.1016/j.jpowsour.2004.08.047.

[7] S. D. Conte y C. de Boor, *Elementary Numerical Analysis: An Algorithmic Approach.*, 2.ª ed. McGraw-Hill.

[8] F. N. Fritsch y R. E. Carlson, «Monotone Piecewise Cubic Interpolation», *SIAM J. Numer. Anal.*, vol. 17, n.º 2, pp. 238-246, 1980.

[9] E. Vairex, «VRB6-25 PERFORMANCE DATA»:.

[10] Li Xiong, Zechang Sun, y Xuezhe Wei, «Modeling and control simulation for fuel cell air supply system», en *2008 IEEE Vehicle Power and Propulsion Conference*, Harbin, Hei Longjiang, China: IEEE, sep. 2008, pp. 1-4. doi: 10.1109/VPPC.2008.4677460.